

Hydrogen effects on crystallinity, photoluminescence, and magnetization of indium tin oxide thin films sputter-deposited on glass substrate without heat treatment

Suning Luo^{1,2}, Shigemi Kohiki^{*1}, Koichi Okada¹, Fumiya Shoji³, and Toetsu Shishido⁴

¹ Department of Materials Science, Kyushu Institute of Technology, Tobata, Sensui 1-1, 804-8550 Kitakyushu, Japan

² Liaoning Institute of Technology, China

³ Kyushu Kyoritsu University, 807-8585 Kitakyushu, Japan

⁴ Institute for Materials Research, Tohoku University, 980-8577 Sendai, Japan

Received ZZZ, revised ZZZ, accepted ZZZ

Published online ZZZ (Dates will be provided by the publisher.)

PACS 68.55.at, 68.35.Dv, 75.20.Ck, 75.70.Ak, 78.55.Hx

* Corresponding author: e-mail kohiki@che.kyutech.ac.jp, Phone: +81-93-884-3310, Fax: +81-93-884-3300

Indium tin oxide (ITO) thin films were sputter deposited by using working gas containing hydrogen on glass substrate without any heat treatments. The films demonstrated x-ray diffraction due to polycrystalline ITO, blue-green photoluminescence (PL) due to oxygen defects in nano-structured ITO crystals, and paramagnetic behaviour in temperature dependence of magnetization overlapped with diamagnetic signal from the substrate. The

carrier density n of the films were of the order of 10^{20} cm^{-3} , and varied as an inverse of V-character with the hydrogen concentration [H] in the gas. The n value peaked at [H] = 1 %. Spectral features at ≈ 430 and ≈ 470 nm of the PL emission were invariant with [H]. The order of the density of electrons N with spins obeying the Curie law was 10^{23} cm^{-3} , and the variation in N with [H] was almost parallel to that in n with [H].

Copyright line will be provided by the publisher

1 Introduction Fabrication of indium tin oxide (ITO) thin films attracts a great attention since it has been the most widely used transparent conducting oxide in semiconductor and electronic device industry [1-3]. ITO thin films with lower resistivity and higher transparency even without heat treatment both in and after deposition are indispensable for next-generation optoelectronic device applications using organic-polymer substrates [4-6]. Either a high substrate temperature in deposition or a post-deposition heating in air at 300 – 500 °C has been believed to oxidize metallic components in the as-deposited film, and then lower the resistivity [7,8].

Shigesato et al. [9] reported that ≤ 90 nm thick films deposited below 100 °C are amorphous. Jun et al. [10] also reported that the film deposited at room temperature RT is almost amorphous, and crystallinity of the film increases as the substrate temperature is increased during deposition.

Such a change in crystallinity resulted from the content of oxygen defects in the films. Since one oxygen deficiency generates two electrons to maintain charge neutrality in ITO crystal, an introduction of hydrogen into the working gas for sputter-deposition is attractive to achieve lower resistivity without any heat treatments. The oxygen defects compensate cation defects and form neutral defects in the crystal [11-13], therefore the hydrogen concentration sufficient for prevailing over the neutral defect formation is obligatory to obtain the as-deposited films with low resistivity.

Hydrogen radical generated in the plasma is a strong reducing species [14]. Therefore, hydrogen in the working gas is anticipated to liberate oxygen from ITO [15], and then to bring about oxygen defects providing n-type carriers of the crystal [16,17]. In crystalline ITO, both Sn^{4+} ions substituted for In^{3+} sites and oxygen vacancy supply carri-

ers at the Fermi level E_F with the density n . Filling in the vacancy with oxygen is reported to cause a rearrangement of atoms, so that preferred (222) orientation is observed in x-ray diffraction [10]. An intense (222) x-ray reflection from the as-deposited film is essential to realize proper concentration of oxygen vacancy for achieving low resistivity.

However, sources of the carriers in amorphous ITO are less clear. It was reported that Sn is not efficiently activated [18]. Carriers are primarily contributed by vacancy-like oxygen defects, but the structure of a vacancy in the amorphous state is still not well defined. Since the electronic properties of ITO clearly depend on the local bonding environment and oxygen defects in oxides are known to exhibit blue-green photoluminescence, the electronic states of oxygen defects in the films can be probed by photoluminescence.

Degenerated n-type carriers at E_F of crystalline ITO are expected to give rise to paramagnetism for the films. The glass substrate is basically diamagnetic, however a lot of oxygen defects included in the substrate also exhibit such a paramagnetic behaviour, therefore paramagnetic Curie constant includes contribution from the film as a variable with the concentration of hydrogen [H] in the gas and that from the substrate as a constant. We can estimate the density of electrons N with spins obeying the Curie law from magnetization measurement. Thus, variation in N with [H] reflects change in the density of oxygen defects of the films. We examined temperature dependence of magnetization of the films, and then compared the variation in N and that in n with [H].

2 Experiment ITO films were deposited on glass substrate without any heat treatments. We used a sintered target (Kojundo Chemical, Japan) with the composition of 95 wt. % In_2O_3 and 5 wt. % SnO_2 for dc sputter-deposition in the working gas containing hydrogen. Deuterium gas (99.99% purity) and argon gas (99.9999% purity) were introduced to deposition chamber of the base pressure $\approx 1 \times 10^{-7}$ Torr. Films were deposited at the hydrogen partial pressures of $\approx 1 \times 10^{-7} - 3.6 \times 10^{-5}$ Torr. The gas pressure ratio of hydrogen to argon, denoted as the hydrogen concentration [H] in the deposition, was in the range of 0 – 3.6 %. The film thickness reached to ≈ 200 nm by deposition of 120 min.

Temperature dependence of resistivity (ρ -T) was measured conventional four probe method. The Hall effects were measured at RT with the van der Pauw method. Platinum electrodes with a thickness of ca. 100 nm were made by a sputtering method on the films, and they were bonded by gold wires to the measurement system. The films were examined by x-ray diffraction (XRD), photoluminescence (PL), and temperature dependence of magnetization (M-T). XRD patterns were measured at RT with a Rigaku CN2013 diffractometer using $\text{Cu K}\alpha$ radiation. PL spectra were measured with a JASCO V-560 spectrometer at RT. M-T was measured by using a Quantum Design

MPMS 5S superconducting quantum interference device magnetometer below 300 K at the field of 100 Oe.

3 Results and discussion As expected for a degenerated system, almost flat ρ -T curve was observed for the films, as shown by the lower panel of Fig. 1. The films of [H] = 1 % and 3.6 % exhibited the lowest ρ and the highest ρ , respectively. From the Hall effects we estimated n and the carrier mobility μ for the films, as shown in the upper panel of Fig. 1. We see an inverse V-shaped behaviour in n peaked at [H] = 1 %, although μ stayed at almost constant below [H] = 1 % and it decreased steeply above [H] = 1 %. A low n and a high μ of the films [H] \leq 1 % suggest that oxygen defects by hydrogen compensated cation defects and formed neutral defects. A high n and a low μ of the films [H] \geq 1 % indicate that oxygen defects by hydrogen were sufficient for prevailing over the neutral defect formation.

In the deposition, hydrogen will decompose In_2O_3 into $\text{In}_2\text{O}_{3-x}$. The ITO films with oxygen vacancies also contain lattice defects such as cation interstitials and Sn^{4+} on In^{3+} sites. The point defects are generally ionized and scatter carriers strongly. It is well known that the ionized impurity scattering is the dominant scattering mechanism in ITO. The defects can be compensated by cation vacancies or associated oxygen clusters, and result in neutral defects. By filling the interstitial positions next to Sn dopants, oxygen vacancy donors ($\text{V}_{\text{O}}^{\bullet}$) neutralize them, and form ($2\text{Sn}_{\text{In}}\text{O}_i^{\bullet}$) associates. The neutral defects also can scatter carriers, however, the neutral impurity scattering is rather poorly understood at present. Carrier scattering mechanisms are still the subject of extensive discussion by now.

As shown by Fig. 2, changes in the XRD patterns with [H] of polycrystalline ITO films are distinguishable. The (400), (440), and (622) reflections were commonly observed for all the films. Especially the (400) reflection was principal for the films [H] = 0.3, 1, and 1.5 %. The (211) reflection was intenser than the other reflections for the [H] = 0 % film. An intense reflection from the (222) plane appeared at first for the film [H] = 1 %, and grew with increasing [H] so as to be the intensest for the film [H] = 3.6 %. The film [H] = 3.6 % demonstrated also the diffuse scattering centred at $2\theta \approx 25^\circ$. It was reported that oxygen vacancies are accommodated preferentially on the (400) plane, and the closest-packed (222) plane does not accommodate vacancies very well and is stabilized when there are fewer oxygen vacancies [10]. The principal (400) reflection indicates that all the films contain a lot of oxygen vacancies in the crystal. Furthermore, the (222) reflection suggests that oxygen vacancies fulfil the role of carrier supplier for the films [H] \geq 1 %. The film [H] = 1 % demonstrated the XRD pattern consisted of the (222), (400), (440), and (622) reflections with almost flat background.

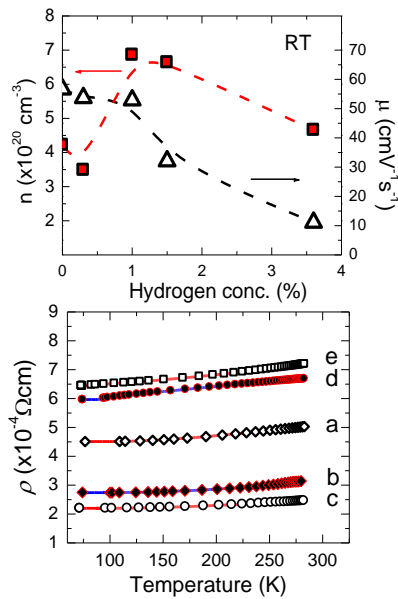


Figure 1 Fig. 1 Lower panel: ρ -T of the films with [H] = 0 (a), 0.3 (b), 1 (c), 1.5 (d), and 3.6 % (e). Upper panel: n and μ of the films at RT versus [H].

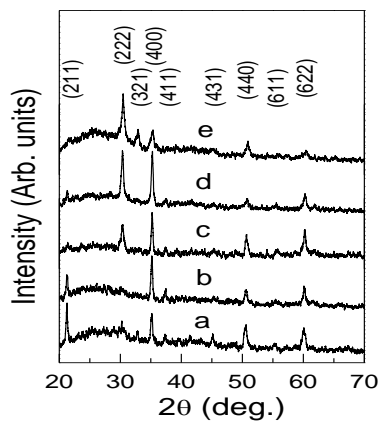


Figure 2 XRD patterns of the films with [H] = 0 (a), 0.3 (b), 1 (c), 1.5 (d), and 3.6 % (e).

While the hydrogen of 1 % in the gas achieved the lowest ρ and the highest transparency, the hydrogen of 3.6 % in the gas brought about higher ρ and lower optical transmittance [11]. It is known that the transmittance is deleteriously affected if the films are too oxygen-deficient as they become more metallic [10]. An intense diffuse scattering at $2\theta \approx 25^\circ$ coexisting with the (222) reflection suggests that the film [H] = 3.6 % is predominantly amorphous and partially crystalline.

It was known that the (400) orientation is dominant for sputter-deposited ITO films while the (222) orientation is the preferred orientation of evaporated ITO films. The ≈ 200 nm-thick ITO films deposited with [H] = 0 and 0.3% indicated the preferred (400) orientation of the sputter-deposition, but those deposited with [H] = 1 and 1.5% demonstrated the preferred (222) orientation of evaporation. With increasing [H] from 0.3 to 1.5%, the (400) orientation peak intensity was depressed, but the (222) orientation peak intensity was enhanced. It was also reported that the small thickness films annealed at 200°C showed a clear (222) peak and a very weak (400) peak with the background almost the same as the as-deposited film. We believed that the appearance of the (222) and even the (400) peaks indicates the formation of In_2O_3 polycrystalline domains during the annealing. The depression of the (400) peak intensity and the enhancement of the (222) peak intensity with [H] indicate the hydrogen effect which enhances growth of In_2O_3 polycrystalline domains even no intentional heat treatment. The crystallinity of the ≈ 200 nm-thick film increased as the hydrogen concentration in the working gas increased.

Despite the variation of [H], all the films demonstrated essentially identical features in the PL spectra, as shown in the lower panel of Fig. 3. The spectra showed a broad peak at ≈ 430 nm (≈ 2.9 eV) with a shoulder at ≈ 470 nm (≈ 2.6 eV).

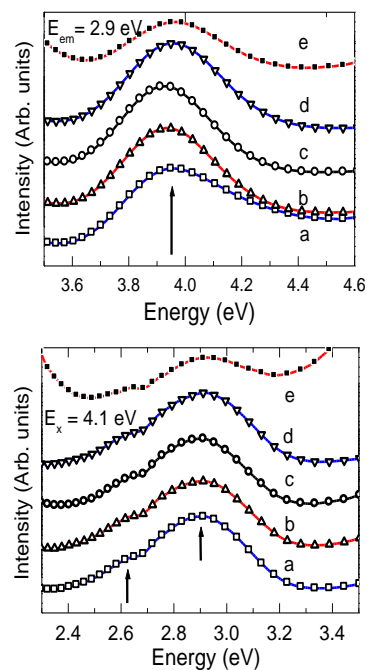


Figure 3 PL (lower panel) and EX (upper panel) spectra measured at RT of the films deposited at [H] = 0 (a), 0.3 (b), 1 (c), 1.5 (d), and 3.6 % (e). The excitation energy E_x for PL was 4.1 eV, and the energy of PL emission E_{em} was 2.9 eV.

It is well known that the stoichiometric In_2O_3 crystal exhibits no PL, while nano-structured In_2O_3 crystal demonstrates a variety of PL. The PL spectra peaked at both 416 and 435 nm [19], at 465 nm [20], and at 470 nm [21] were reported for nano-wires, and that peaked at 470 nm was reported for both nano-pyramids and nano-columns [22] and for nano-fibers [23]. The PL spectra peaked at both 480 and 520 nm were reported for nano-particles [24]. There are also reports of the 470 nm PL for bulk powders [25], and the 637 nm PL for the films heated above 800 °C for 1 h in oxygen ambient [26]. Such PL is resulted from radiative recombination of electrons trapped by holes on oxygen defects. The oxygen defects are anticipated to add the electronic states of the oxygen defects in the bandgap. The excitation EX spectra corresponding to the observed PL peak at ≈ 2.9 eV (≈ 430 nm) exhibited a broad peak centred at 3.95 eV for all the films regardless of the variation in [H]. The optical bandgap of $\sim 3.5 - 4.0$ eV has been reported for ITO [27,28]. The PL and EX spectra revealed that the electronic states created by hydrogen are essentially the same notwithstanding the variation of [H], and the observed PL can be attributed to the deep-level emission due to the oxygen defects in nano-structured ITO crystals of the polycrystalline films. The PL spectrum of the film [H] = 3.6 % is apparently less intense than the other is, which is consistent to the fact in XRD that the film is predominantly amorphous and partially crystalline.

Susceptibility as a function of inverse temperature ($\chi \cdot T^{-1}$) of the films on the substrate was shown in the lower panel of Fig. 4. The negative sign for χ is brought about by diamagnetism of the substrate. The $\chi \cdot T^{-1}$ curves demonstrated positive slope for χ with increasing T^{-1} , and are represented well by straight lines obtained from the least square fitting. The slope of χ can be converted to N for each film. It is known that susceptibility of the Curie paramagnetism can be written as $\chi = N\mu_0\mu^2/3k_B T$. Where N is the density of spins obeying the Curie law, μ_0 is the permeability of free space, μ is the magnetic moment of a spin obeying the Curie law, and k_B is the Boltzmann constant. Here, we assumed that $\mu = 1 \mu_B$ (the Bohr magneton). The N value estimated from the $\chi \cdot T^{-1}$ curve for the films are shown in the upper panel of Fig. 4. The N value derived from the $\chi \cdot T^{-1}$ slope demonstrated an inverse V-shaped behaviour with the [H] value. The largest N value was achieved at [H] = 1 %, where the resistivity was the lowest. The variation in N with [H] looks rather parallel to that in n with [H]. The weakest diffuse scattering at $2\theta \approx 25^\circ$ coexisting with both the (222) and (400) reflections in XRD corresponded well to the largest N and n of the film [H] = 1 %. The order of N was 10^{23} cm^{-3} but that of n was 10^{20} cm^{-3} . Therefore, almost all the electrons with spins obeying the Curie law are located in the glass substrate, however not a few electrons activated to E_F of crystalline ITO exhibited an inverse V-shaped behaviour with [H].

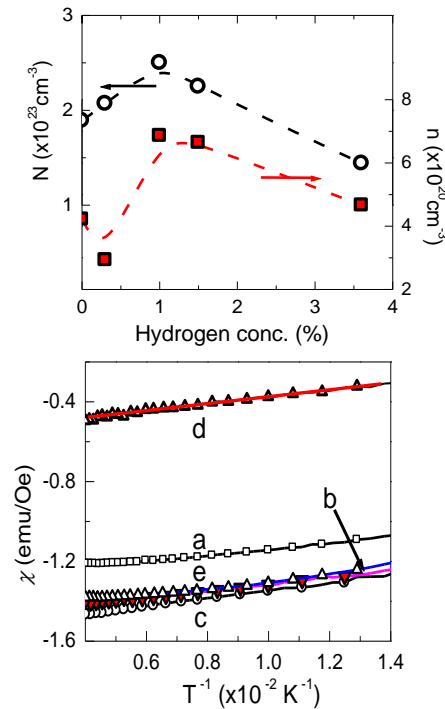


Figure 4 Lower panel: $\chi \cdot T^{-1}$ measured at $H = 100$ Oe of the films deposited at [H] = 0 (a), 0.3 (b), 1 (c), 1.5 (d), and 3.6 % (e) on the substrate. The straight (red) line for $\chi \cdot T^{-1}$ of the film d is shown in the figure as an example of the least square fitting.

Upper panel: magnetically estimated N and n of the films versus [H].

4 Summary Sputter-deposited ITO films with [H] = 0, 0.3, 1, 1.5, and 3.6 % were examined by XRD, PL, and M-T. The x-ray intensity of diffuse scattering at $2\theta \approx 25^\circ$ coexisting with the (222) and/or (400) reflections for the film with [H] = 1 % and that for the film with [H] = 3.6 % were the weakest and the strongest, respectively. The electronic states of the oxygen defects are the same for crystalline ITO of the films since the spectral features at ≈ 430 and ≈ 470 nm of PL were commonly observed for all the films. The strongest x-ray diffuse scattering at $2\theta \approx 25^\circ$ corresponded well to the weakest PL for the film with [H] = 3.6 %. The N value derived from the M-T curve showed an inverse V-shaped behaviour peaked at [H] = 1 %. The order of the N value of each film was 10^{23} cm^{-3} , and the variation in N with [H] was almost parallel to that in n with [H] of the order of 10^{20} cm^{-3} . Such parallelism between N and n suggests that magnetization measurement is applicable to evaluate concentration of the oxygen defects by hydrogen in the gas.

Acknowledgements The authors thank Dr. H. Shimooka for assistance in this work. A part of this work was performed under the inter-university cooperative research program of the

1 Advanced Research Centre of Metallic Glasses, Institute for Ma-
2 terials Research, Tohoku University.

3 4 **References**

- 5 [1] A. Salehi, *Thin Solid Films* **324**, 214 (1998).
6 [2] J. K. Sheu, Y. K. Su, G. C. Chi, M. J. Jou, and C. M. Chang,
7 *Appl. Phys. Lett.* **72**, 3317 (1998).
8 [3] B. Lewis and D. Paine, *MRS Bulletin* **25**, 22 (2000).
9 [4] D. Ginley and C. Bright, *MRS Bulletin* **25**, 15 (2000).
10 [5] C. G. Granqvist and A. Hultaker, *Thin Solid Films* **411**, 1
11 (2002).
12 [6] S. Lany and A. Zunger, *Phys. Rev. Lett.* **98**, 045501 (2007).
13 [7] R. X. Wang, C. D. Beling, S. Fung, A. B. Djurisic, C. C.
14 Ling, and S. Li, *J. Appl. Phys.* **97**, 033504 (2005).
15 [8] R. X. Wang, C. D. Beling, S. Fung, A. B. Djurisic, C.
16 Kwong, and S. Li, *J. Phys. D: Appl. Phys.* **38**, 2000 (2005).
17 [9] Y. Shigesato, R. Koshi-ishi, T. Kawashima, and J. Ohsako,
18 *Vacuum* **59**, 614 (2000).
19 [10] S. -I. Jun, T. E. McKnight, M. L. Simpson, and P. D. Rack,
20 *Thin Solid Films* **476**, 59 (2005).
21 [11] S. Luo, K. Okada, S. Kohiki, F. Tsutsui, H. Shimooka, and F.
22 Shoji, *Materials Letters* **63**, 641 (2009).
23 [12] S. Ishibashi, Y. Higuchi, Y. Ota, and K. Nakamura, *J. Vac.*
24 *Sci. Technol. A* **8**, 1399 (1990).
25 [13] S. N. Luo, A. Kono, N. Nouchi, and F. Shoji, *J. Appl. Phys.*
26 **100**, 113701 (2006).
27 [14] J. Wallinga, W. M. Arnold Bik, A. M. Vredenberg, R. E. I.
28 Schropp, and W. F. van der Weg, *J. Phys. Chem. B* **102**,
29 6219 (1998).
30 [15] R. Banerjee, S. Ray, N. Basu, A. K. Batabyal, and A. K. Ba-
31 rua, *J. Appl. Phys.* **62**, 912 (1987).
32 [16] J. H. W. Dewit, *J. Solid State Chem.* **8**, 142 (1973).
33 [17] J. H. W. Dewit, G. Vanunen, and M. Lahey, *J. Phys. Chem.*
34 *Solids* **38**, 819 (1977).
35 [18] H. Morikawa and M. Fujita, *Thin Solid Films* **359**, 61 (2000).
36 [19] X. C. Wu, J. M. Hong, Z. J. Han, and Y. R. Tao, *Chem. Phys.*
37 *Lett.* **373**, 28 (2003).
38 [20] M. J. Zheng, L. D. Zhang, G. H. Li, X. Y. Zhang, and X. F.
39 Wang, *Appl. Phys. Lett.* **79**, 839 (2001).
40 [21] S. Kar and S. Chaudhuri, *Chem. Phys. Lett.* **422**, 424 (2006).
41 [22] P. Guha, S. Kar, and S. Chaudhari, *Appl. Phys. Lett.* **85**,
42 3851 (2004).
43 [23] C. H. Liang, G. W. Meng, Y. Lei, F. Phillipp, and L. D.
44 Zhang, *Adv. Mater.* **13**, 1330 (2001).
45 [24] H. J. Zhou, W. P. Cai, and L. D. Zhang, *Appl. Phys. Lett* **75**,
46 495 (1999).
47 [25] L. Dai, X. L. Chen, J. K. Jian, M. He, T. Zhou, and B. Q. Hu,
48 *Applied physics A* **75**, 687 (2002).
49 [26] M-S. Lee, W. C. Choi, E. K. Kim, C. K. Kim, and S-K Min,
50 *Thin Solid Films* **279**, 1 (1996).
51 [27] J. C. C. Fan, J. B. Goodenough, *J. Appl. Phys.* **48**, 3524
52 (1977).
53 [28] N. Balasubramanian and A. Subrahmanyam, *J. Phys. D* **22**,
54 206 (1989).
55
56
57